

C.P. No. 486
(21,387)
A.R.C. Technical Report

C.P. No. 486
(21,387)
A.R.C. Technical Report



MINISTRY OF AVIATION

AERONAUTICAL RESEARCH COUNCIL

CURRENT PAPERS

Calculation of the Recoil of a Shock Tube

by

F/Lt. B. A. Woods, R.N.Z.A.F.

LONDON: HER MAJESTY'S STATIONERY OFFICE

1960

PRICE 2s. 6d. NET

U.D.C. No. 533.6.073

Technical Note No. Aero 2627

June, 1959

R O Y A L A I R C R A F T E S T A B L I S H M E N T

CALCULATION OF THE RECOIL OF A SHOCK TUBE

by

B. A. Woods (Flt. Lt. R.N.Z.A.F.)

SUMMARY

The method for calculating the unsteady pressure force acting on the high pressure end of a shock tube after the rupture of the diaphragm is set out. The mathematical development, using a solution due to Riemann, is taken from Courant and Friedrichs¹. For air or hydrogen ($\gamma = 7/5$) a simple closed expression for the pressure is obtained, and the first and second integrals of this with respect to time are given. It is shown how these permit one to estimate the recoil of a typical dynamical system. Calculated pressures are found to be in good agreement with a set of experimental results.

LIST OF CONTENTS

	<u>Page</u>
LIST OF SYMBOLS	3
1 INTRODUCTION	4
2 DYNAMICS OF THE SYSTEM	4
3 VARIATION OF PRESSURE AT THE CLOSED END OF THE HIGH PRESSURE CHAMBER	5
4 INTEGRALS OF PRESSURE WITH RESPECT TO TIME	7
5 COMPARISON OF THEORETICAL AND EXPERIMENTAL VARIATIONS OF PRESSURE WITH TIME	8
LIST OF REFERENCES	9
TABLE 1 - Values of $\frac{p}{p_0}$, $\frac{t}{t_0}$, f and g	10
ILLUSTRATIONS - Figs.1-5	-

LIST OF ILLUSTRATIONS

	<u>Fig.</u>
Diagram of shock tube installation, showing forces governing recoil	1
Characteristic diagram showing interaction between incident (s) and reflected (r) waves	2
Variation of $\frac{p}{p_0}$ and g with time	3
Variation of f with time	4
Comparison of theoretical and experimental variations of pressure (at closed end of tube) with time (experimental results from R.A.E. 6 inch high pressure shock tube)	5

LIST OF SYMBOLS

a	local speed of sound
A	cross sectional area of shock tube
$f\left(\frac{t}{t_0}\right), g\left(\frac{t}{t_0}\right)$	first and second integrals of unsteady pressure force, defined by equation (2)
g	gravitational acceleration
M_1, M_2	masses of the high pressure chamber and of the buffer block
p	pressure
r, s	Riemann variables, equation (3)
R	retarding force on M_1
t	time
u	one-dimensional flow velocity
x	distance along the tube (used for displacement of tube)
X	reaction between masses M_1 and M_2
y	defined by (8)
z	used in definition of hypergeometric function, section 3
γ	ratio of specific heats of driver gas
λ	$\frac{(\gamma + 1)}{2(\gamma - 1)}$
μ	coefficient of friction
Suffix o	refers to the initial conditions before the arrival of the head of the expansion at the closed end of the tube

1 INTRODUCTION

When the diaphragm in a shock tube is ruptured, the high pressure section is subjected to an unbalanced force due to the pressure acting on the closed end, and will, if not rigidly mounted, be displaced a distance backwards. The purpose of the present note is to show how this displacement may be estimated. It depends primarily on

- (i) the magnitude of the pressure force, and the time for which it acts,
- (ii) the mass of the driving end of the tube, and the retarding forces in the system.

The dynamical equations for a typical system are set out in section 2, and it is seen that the displacement depends on the way the pressure on the closed end varies with time; the solution for this is given in section 3 and its first and second integrals with respect to time in section 4. Pressures calculated by the formula of section 3 are compared with a set of experimental values in section 5 and good agreement is found.

2 DYNAMICS OF THE SYSTEM

In the design of a shock tube installation, constraints may be introduced to resist displacement due to the unsteady load in a variety of ways. The retarding force may be constant, a function of t , x , dx/dt , or of a combination of these. It may be necessary to consider two or more components, and in the scheme proposed for the R.A.E. 6 inch High Pressure Shock Tube, shown diagrammatically in Fig. 1, the retarding force R , (acting on the high-pressure chamber M_1) is due, for example, to a precompressed spring of very high hysteresis and so may be regarded as constant, and is of such magnitude that during the recoiling motion, the two masses M_1 and M_2 of the high-pressure chamber and of the buffer block separate. To describe the motion fully, it is convenient to introduce the force of reaction between the two masses, X . Then the equations of motion for each component of the system are

$$\left. \begin{aligned} M_2 \frac{d^2 x_2}{dt^2} &= X - \mu M_2 g \\ M_1 \frac{d^2 x_1}{dt^2} &= p(t) A - R - X \end{aligned} \right\} \quad (1)$$

where A is the cross sectional area and p the pressure on the end of the tube. For $X > 0$, i.e. before separation, $x_1 = x_2$ and the equations may be combined to give

$$(M_1 + M_2) \frac{d^2 x}{dt^2} = p(t) A - R - \mu M_2 g \quad (1a)$$

but when $X = 0$, i.e. at and after the time t , such that

$$p(t_1) A + \mu M_2 g - R = 0, \quad (1b)$$

the displacements x_1 and x_2 of the masses M_1 and M_2 become distinct, and the two equations must be used, with $X = 0$.

The integration of the equation of motion (1) is straightforward, although if $p(t)$ and R are not given as simple functions of t or x , it may have to be done numerically. In the remainder of this note, an expression is obtained for p/p_0 as a function of t/t_0 , where p_0 is the initial pressure in the driver and t_0 is the time that elapses between the rupture of the diaphragm and the arrival of the head of the expansion fan at the closed end of the high pressure chamber. (For $t \leq t_0$, $p = p_0$.)

This expression is then integrated to give the functions

$$f\left(\frac{t}{t_0}\right) \equiv \int_0^{\frac{t}{t_0}} \frac{p}{p_0} d\left(\frac{t}{t_0}\right)$$

and

$$g\left(\frac{t}{t_0}\right) \equiv \int_0^{\frac{t}{t_0}} f d\left(\frac{t}{t_0}\right)$$
(2)

which represent the contributions of the unsteady pressure to the velocity and displacement of the tube, for the case where the expanding gas in the high pressure chamber has the constant specific heat ratio $\gamma = 1.4$.

3 VARIATION OF PRESSURE AT THE CLOSED END OF THE HIGH PRESSURE CHAMBER

The pressure-time history at the closed end of the tube is found from a solution for the reflection at a rigid wall of the centred rarefaction wave travelling upstream from the diaphragm. This is given in section 82 of Courant and Friedrichs¹, and outlined here.

The equations of motion and continuity of a one-dimensional unsteady isentropic flow may be written in the form

$$\left. \begin{aligned} r &= \frac{2a}{\gamma-1} + u = \text{const. along a line } \frac{dx}{dt} = u + a \\ s &= \frac{2a}{\gamma-1} - u = \text{const. along a line } \frac{dx}{dt} = u - a \end{aligned} \right\} \quad (3)$$

The r and s characteristics are indicated in Fig.2. r is constant throughout the region unaffected by the reflection, in which region the flow is a "simple wave". At the end wall $u = 0$, so that at any time t $r_{\text{wall}} = s_{\text{wall}}$ and, with the notation of Fig.2, $r_1 = s_1$, $r_2 = s_2$ etc.

Within the region of interaction, by (3)

$$\frac{\partial x}{\partial s} = (u + a) \frac{\partial t}{\partial s} \quad , \quad \frac{\partial x}{\partial r} = (u - a) \frac{\partial t}{\partial r} \quad . \quad (4)$$

Thus, eliminating x and putting u and a in terms of r and s , we obtain

$$\frac{\partial^2 t}{\partial r \partial s} + \frac{\lambda}{r+s} \frac{\partial t}{\partial r} + \frac{\partial t}{\partial s} = 0 \quad (5)$$

where

$$\lambda = \frac{(\gamma + 1)}{2(\gamma - 1)} \quad (6)$$

The solution of this equation which satisfies the boundary conditions imposed by the initial centred nature of the incident wave, and by the reflection at the wall is*

$$t(r, s) = t_0 \left(\frac{r_0 + s_0}{r + s} \right)^\lambda F(1 - \lambda, \lambda; 1; -y) \quad (7)$$

where

$$y = \frac{(r_0 - r)(s_0 - s)}{(r_0 + s_0)(r + s)} \quad (8)$$

F is the hypergeometric function, defined by

$$F(a, b; c; z) = 1 + \frac{a \cdot b}{c \cdot 1!} z + \frac{a(a+1) b(b+1)}{c(c+1) 2!} z^2 + \dots,$$

and t_0 is the time at which the incident wave first meets the end of the tube. At the end of the tube $r = s = 2a/(\gamma - 1)$, where a is the local speed of sound at time t ; thus by (7) a and t are connected by

$$t(a) = t_0 \left(\frac{a_0}{a} \right)^\lambda F(1 - \lambda, \lambda; 1; -y), \quad (9)$$

where

$$x = \frac{\left(1 - \frac{a}{a_0}\right)^2}{4\left(\frac{a}{a_0}\right)}, \quad (10)$$

a_0 being the initial speed of sound in the undisturbed driver.

*This may be verified by assuming a solution of the form

$$\frac{t}{t_0} = \left(\frac{r_0 + s_0}{r + s} \right)^\lambda F(y),$$

in which case a second-order linear equation is obtained for F which may be solved in series. A fuller account is given by Steketee².

The hypergeometric function reduces to a polynomial of degree $\lambda - 1$ when λ is a positive integer. This is so whenever γ is of the form $(2n + 3)/(2n + 1)$, as is the case for polyatomic gases. Thus for a monatomic gas ($\gamma = 5/3$) we should have $F \equiv 1 + 2x$, while for hydrogen or air which are diatomic, ($\gamma = 7/5$), we have the quadratic expression

$$F(-2, 3; 1; -y) = 1 + 6y + 6y^2 \quad (11)$$

The pressure is given in terms of the speed of sound by $\frac{a}{a_0} = \left(\frac{p}{p_0}\right)^{\frac{\gamma-1}{2\gamma}} = \left(\frac{p}{p_0}\right)^{1/7}$.

The last three equations enable us to write the pressure-time history at the end of the tube as

$$\left. \begin{aligned} 0 < t < t_0, & \quad p = p_0 \\ t_0 < t, & \quad \frac{t}{t_0} = \frac{3}{8} \left(\frac{p}{p_0}\right)^{-5/7} + \frac{1}{4} \left(\frac{p}{p_0}\right)^{-3/7} + \frac{3}{8} \left(\frac{p}{p_0}\right)^{-1/7} \end{aligned} \right\} \quad (12)$$

4 INTEGRALS OF PRESSURE WITH RESPECT TO TIME

The integrals defined by equation (2) which give the contributions of the unsteady pressure to the velocity and displacement of the system may now be calculated, using (12). The first is

$$f\left(\frac{t}{t_0}\right) = \int_0^{\frac{t}{t_0}} \left(\frac{p}{p_0}\right) d\left(\frac{t}{t_0}\right)$$

$$\left. \begin{aligned} \text{For} & \quad 0 < \frac{t}{t_0} < 1 & \quad f\left(\frac{t}{t_0}\right) = \frac{t}{t_0} \\ \text{and for} & \quad \frac{t}{t_0} > 1 & \quad 16 f\left(\frac{t}{t_0}\right) = 35 - 15 \left(\frac{p}{p_0}\right)^{2/7} - 3 \left(\frac{p}{p_0}\right)^{4/7} - \left(\frac{p}{p_0}\right)^{6/7} \end{aligned} \right\} \quad (13)$$

From this the second integral, defined by

$$g\left(\frac{t}{t_0}\right) = \int_0^{\frac{t}{t_0}} f\left(\frac{t}{t_0}\right) d\left(\frac{t}{t_0}\right)$$

is found as

$$g\left(\frac{t}{t_0}\right) = \frac{1}{2} \left(\frac{t}{t_0}\right)^2$$

for

$$0 \leq \frac{t}{t_0} \leq 1, \text{ and}$$

$$16 g\left(\frac{t}{t_0}\right) = \frac{105}{8} \left(\frac{p}{p_0}\right)^{-5/7} - \frac{5}{8} \left(\frac{p}{p_0}\right)^{-3/7} - \frac{15}{4} \left(\frac{p}{p_0}\right)^{-1/7} + \frac{39}{4} \left(\frac{p}{p_0}\right)^{1/7} + \frac{5}{8} \left(\frac{p}{p_0}\right)^{3/7} + \frac{3}{40} \left(\frac{p}{p_0}\right)^{5/7} - \frac{56}{5}$$

(14)

for $\frac{t}{t_0} > 1$.

p/p_0 , f and g are tabulated for $t/t_0 > 1$ in Table 1 and plotted in Figs.3 and 4.

5 COMPARISON OF THEORETICAL AND EXPERIMENTAL VARIATIONS OF PRESSURE WITH TIME

Fig.5 compares pressures calculated from equation 12 with measurements (unpublished) made at the closed end of the R.A.E. 6 inch High Pressure Shock Tube, for a particular operating condition with hydrogen driver at 2,300 p.s.i. and 290°K. The experimental results were obtained with an SIM PZ 14 pressure transducer.

The experimental value of t_0 was 7.0 milliseconds. This agrees with the time that would be calculated for the head of the expansion fan to travel the 30 ft from the diaphragm to the closed end of the high pressure chamber, assuming that it moves at the speed of sound in hydrogen at 290°K, namely 4270 feet per second.

After that, there is extremely good agreement between experiment and theory, at least up to times between 35 and 40 milliseconds after rupture of the diaphragm, when the pressure has dropped below 100 p.s.i. (compared with the initial value of 2,300 p.s.i.).

For times in excess of 40 milliseconds, the experimental results drop below the theoretical curve. The reason for this is not yet understood; it may be fundamental, or arise from experimental error, or be a combination of both.

However, with the exception of the long drawn out "tail" of the theoretical estimate (note that Fig.5 covers only the region up to $t/t_0 = 8$ of Fig.3) the comparison would indicate that the theoretical formulae of this note may be applied with fair confidence to the calculation of the recoil of a shock tube.

LIST OF REFERENCES

<u>Ref. No.</u>	<u>Author</u>	<u>Title, etc.</u>
1	Courant, R. Fredrichs, K.O.	Supersonic flow and shock waves. Interscience Publishers, Inc. New York (1948)
2	Steketee, J.A.	On the interaction of rarefaction waves in a shock tube. University of Toronto Institute of Aerophysics, Review No.4 (1952)

TABLE 1

Values of $\frac{p}{p_0}$, $\frac{t}{t_0}$, f and g

$\frac{p}{p_0}$	$\frac{t}{t_0}$	f	g
1.0	1.0	1.000	0.5
0.9	1.046		
0.8	1.102	1.0912	0.609
0.7	1.169		
0.6	1.255	1.1969	0.784
0.5	1.366		
0.4	1.520	1.3264	1.119
0.3	1.750		
0.2	2.139	1.5051	2.024
0.15	2.53		
0.1	3.14	1.6429	3.574
0.08	3.540	1.6805	4.270
0.075	3.69		
0.06	4.194	1.725	5.359
0.05	4.67		
0.04	5.336	1.780	7.344
0.02	8.123	1.859	12.45
0.013	10.65	1.9061	17.09
0.012	11.20	1.9103	18.13
0.010	12.58	1.9213	20.89
0.009	13.46	1.9296	22.59
0.008	14.53	1.9384	25.64
0.007	15.84	1.9485	27.19
0.006	17.51	1.9593	30.46
0.005	19.23	1.9714	34.82
0.004	22.84	1.9854	40.99
0.003	27.65	2.0020	50.56
0.002	36.26	2.0230	67.89
0.001	57.94	2.0534	112.1

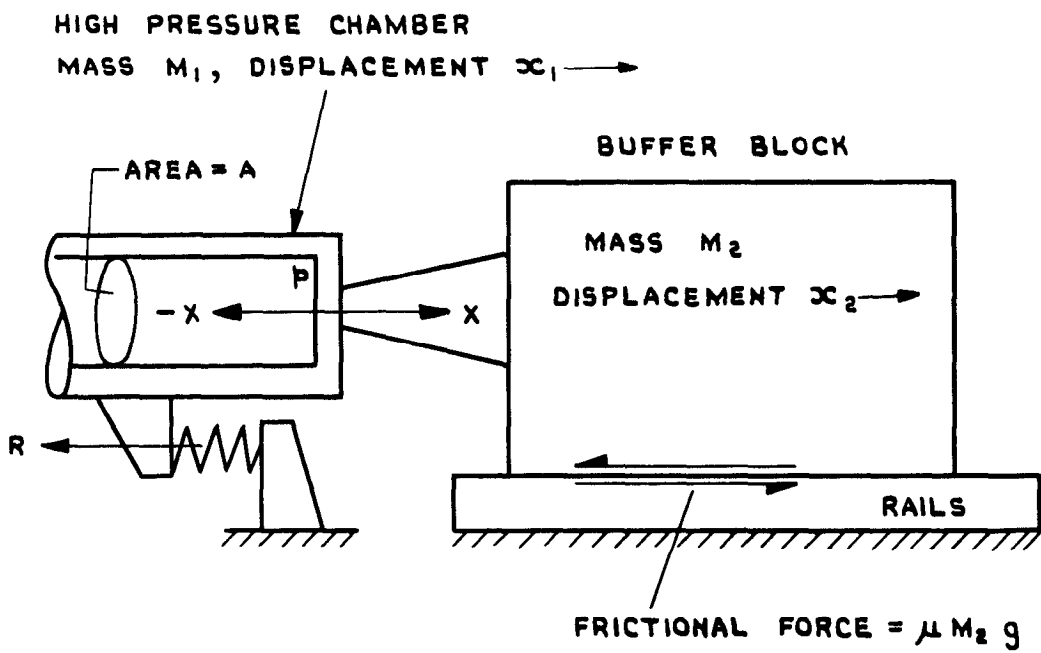


FIG. I. DIAGRAM OF SHOCK TUBE INSTALLATION,
 SHOWING FORCES GOVERNING RECOIL.

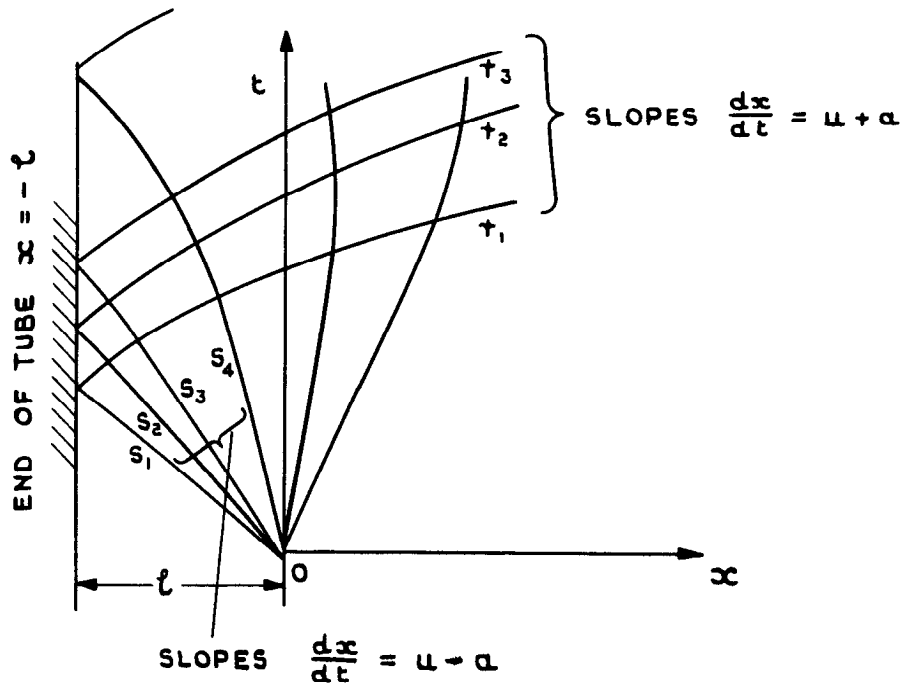


FIG. 2. CHARACTERISTIC DIAGRAM SHOWING INTERACTION BETWEEN INCIDENT (s) AND REFLECTED (r) WAVES.

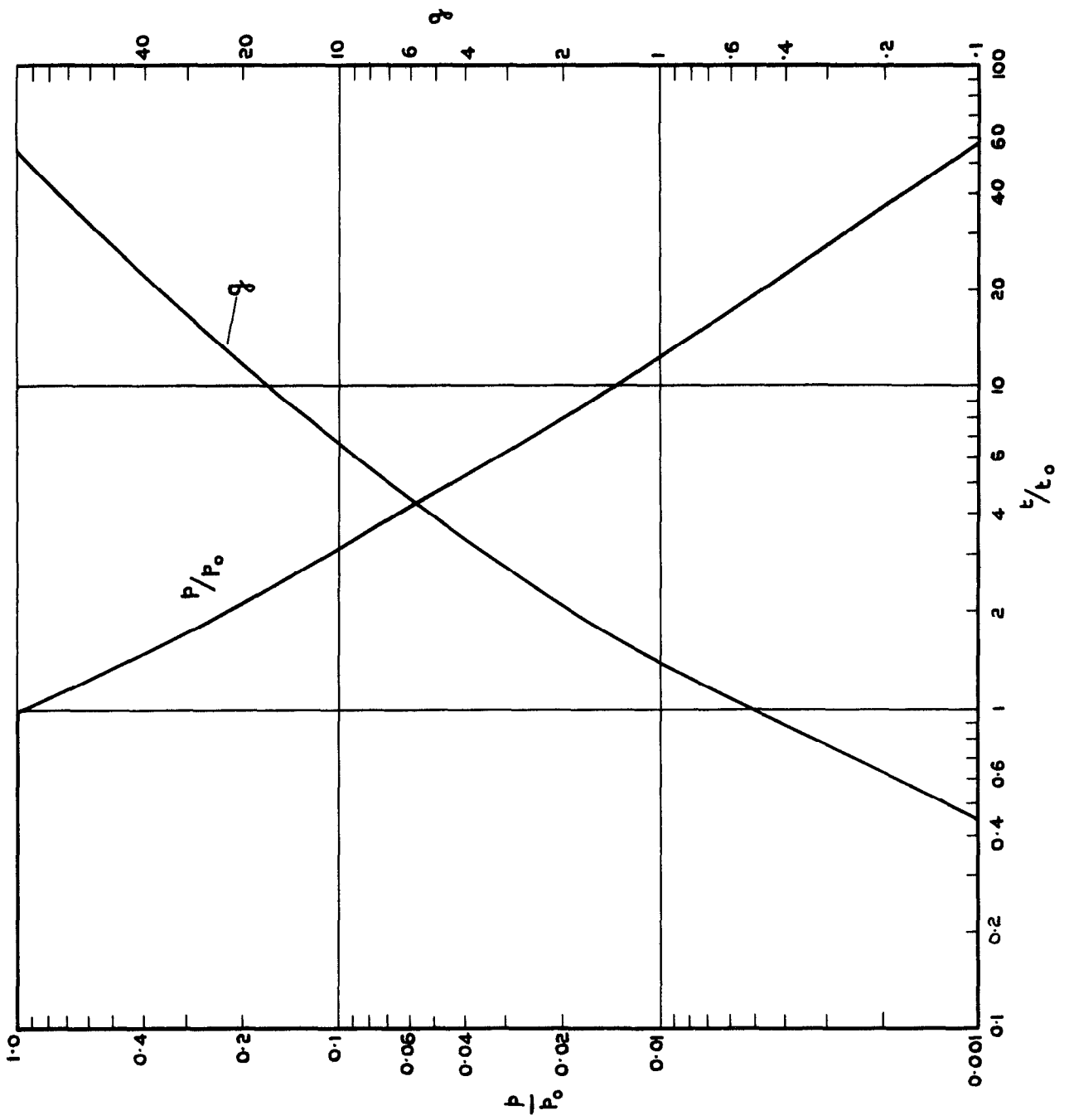


FIG. 3. VARIATION OF P/P_0 AND q WITH TIME.

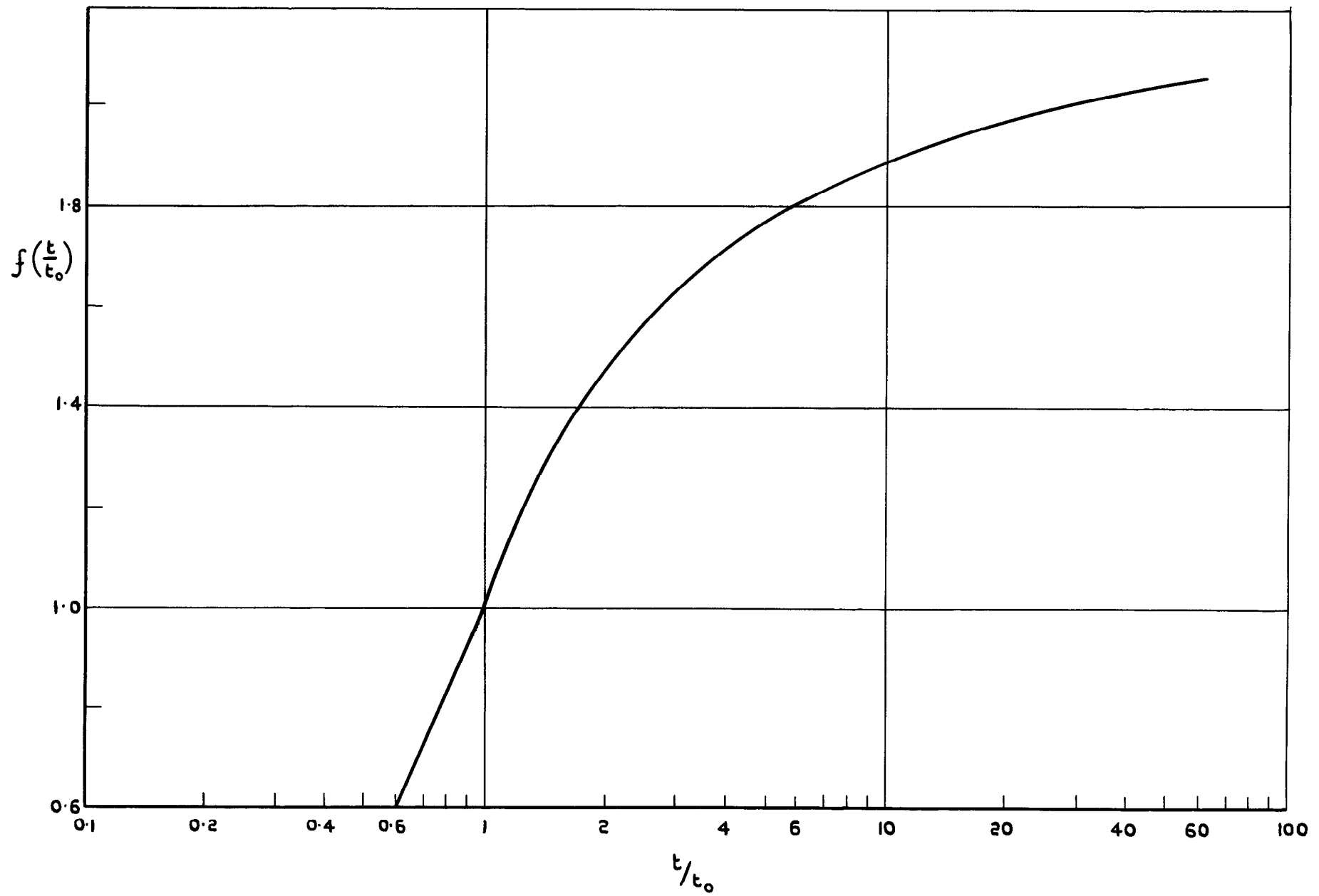


FIG. 4. VARIATION OF f WITH TIME.

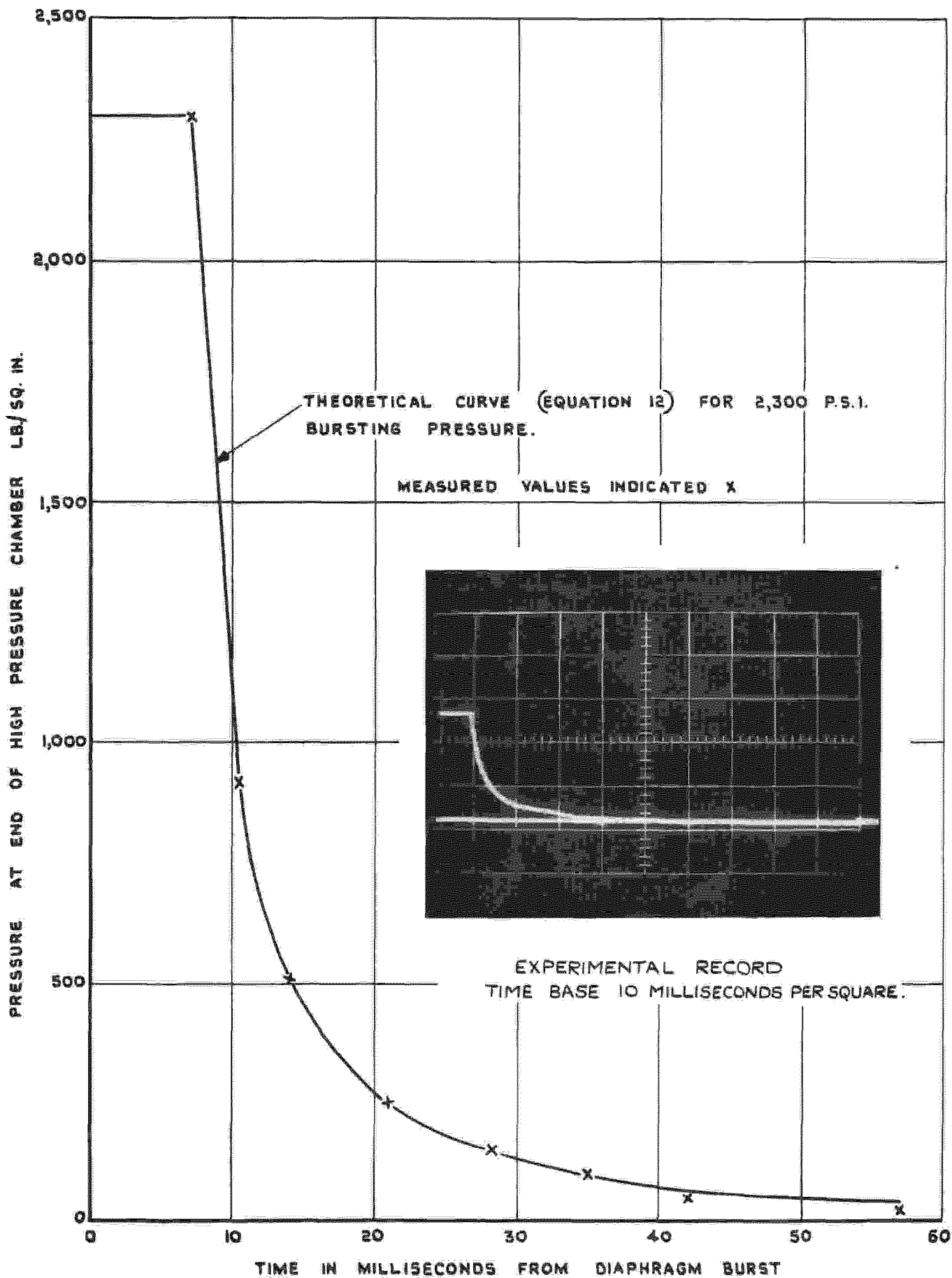


FIG. 5. COMPARISON OF THEORETICAL AND EXPERIMENTAL VARIATIONS OF PRESSURE (AT CLOSED END OF TUBE) WITH TIME.

© *Crown Copyright 1960*

Published by
HER MAJESTY'S STATIONERY OFFICE

To be purchased from
York House, Kingsway, London W.C.2
423 Oxford Street, London W.1
13A Castle Street, Edinburgh 2
109 St. Mary Street, Cardiff
39 King Street, Manchester 2
Tower Lane, Bristol 1
2 Edmund Street, Birmingham 3
80 Chichester Street, Belfast
or through any bookseller

Printed in England